Integrated Environmental Assessment and Management — Volume 17, Number 4—pp. 705–715
Received: 16 October 2020 | Returned for Revision: 25 January 2021 | Accepted: 16 March 2021

Special Series

The impact of precursors on aquatic exposure assessment for PFAS: Insights from bioaccumulation modeling

David Glaser,[1] Elizabeth Lamoureux,[1] Dan Opdyke,[2] Sarah LaRoe,[3] Deirdre Reidy,[4] and John Connolly[1]
[1]*Anchor QEA LLC, Woodcliff Lake, New Jersey, USA*
[2]*Anchor QEA LLC, Austin, Texas, USA*
[3]*Anchor QEA LLC, Saratoga Springs, New York, USA*
[4]*Anchor QEA LLC, Liverpool, New York, USA*

EDITOR'S NOTE:

This article is part of the special series "Ecological Risk Assessment for Per- and Polyfluorinated Alkyl Substances." The series documents and advances the current state of the practice, with respect to ecotoxicological research, environmental exposure monitoring and modeling, ecologically based screening benchmarks, and risk assessment frameworks.

Abstract

Risk assessment for per- and polyfluoroalkyl substances (PFAS) is complicated by the fact that PFAS include several thousand compounds. Although new analytical methods have increased the number that can be identified in environmental samples, a significant fraction of them remain uncharacterized. Perfluorooctane sulfonate (PFOS) is the PFAS compound of primary interest when evaluating risks to humans and wildlife owing to the consumption of aquatic organisms. The exposure assessment for PFOS is complicated by the presence of PFOS precursors and their transformation, which can occur both in the environment and within organisms. Thus, the PFOS to which wildlife or people are exposed may consist of PFOS that was discharged directly into the environment and/or other PFOS precursors that were transformed into PFOS. This means that exposure assessment and the development of remedial strategies may depend on the relative concentrations and properties not only of PFOS but also of other PFAS that are transformed into PFOS. A bioaccumulation model was developed to explore these issues. The model embeds toxicokinetic and bioenergetic components within a larger food web calculation that accounts for uptake from both food and water, as well as predator–prey interactions. Multiple chemicals are modeled, including parent–daughter reactions. A series of illustrative simulations explores how chemical properties can influence exposure assessment and remedial decision making. *Integr Environ Assess Manag* 2021;17:705–715. © 2021 The Authors. *Integrated Environmental Assessment and Management* published by Wiley Periodicals LLC on behalf of Society of Environmental Toxicology & Chemistry (SETAC).

KEYWORDS: Bioaccumulation, Model, PFAS, PFOS, Precursor

INTRODUCTION

Per- and polyfluoroalkyl substances (PFAS) are environmental contaminants of increasing regulatory interest owing to concerns over potential adverse impacts on human health and the environment. Drinking water criteria have been established in various jurisdictions for a subset of PFAS, in particular perfluoroalkyl acids (PFAAs) such as perfluorooctane sulfonate (PFOS) and perfluorooctanoic acid (PFOA; ITRC, 2020a). Levels to protect human health have also been established for PFOS in fish, including fish consumption advisories (e.g., Minnesota [MDH, 2018]) and Environmental Quality Standards in the European Union (EU, 2013).

PFAS include thousands of chemicals (OECD, 2018), some of which (termed PFAA precursors) transform in the environment and in vivo to PFAAs, such as PFOS, which is not known to transform further (ITRC, 2020b). PFOS has been shown to bioaccumulate in fish (e.g., Martin et al., 2003a, 2003b), wildlife (Boisvert et al., 2019), and humans (ITRC, 2020b). It exists mostly as an anion in the environment and exhibits a low partition coefficient, with values for the log sediment partition coefficient ranging

Correspondence David Glaser, Anchor QEA LLC, Woodcliff Lake, NJ, USA.
Email: dglaser@anchorqea.com

Published 24 March 2021 on wileyonlinelibrary.com/journal/ieam.

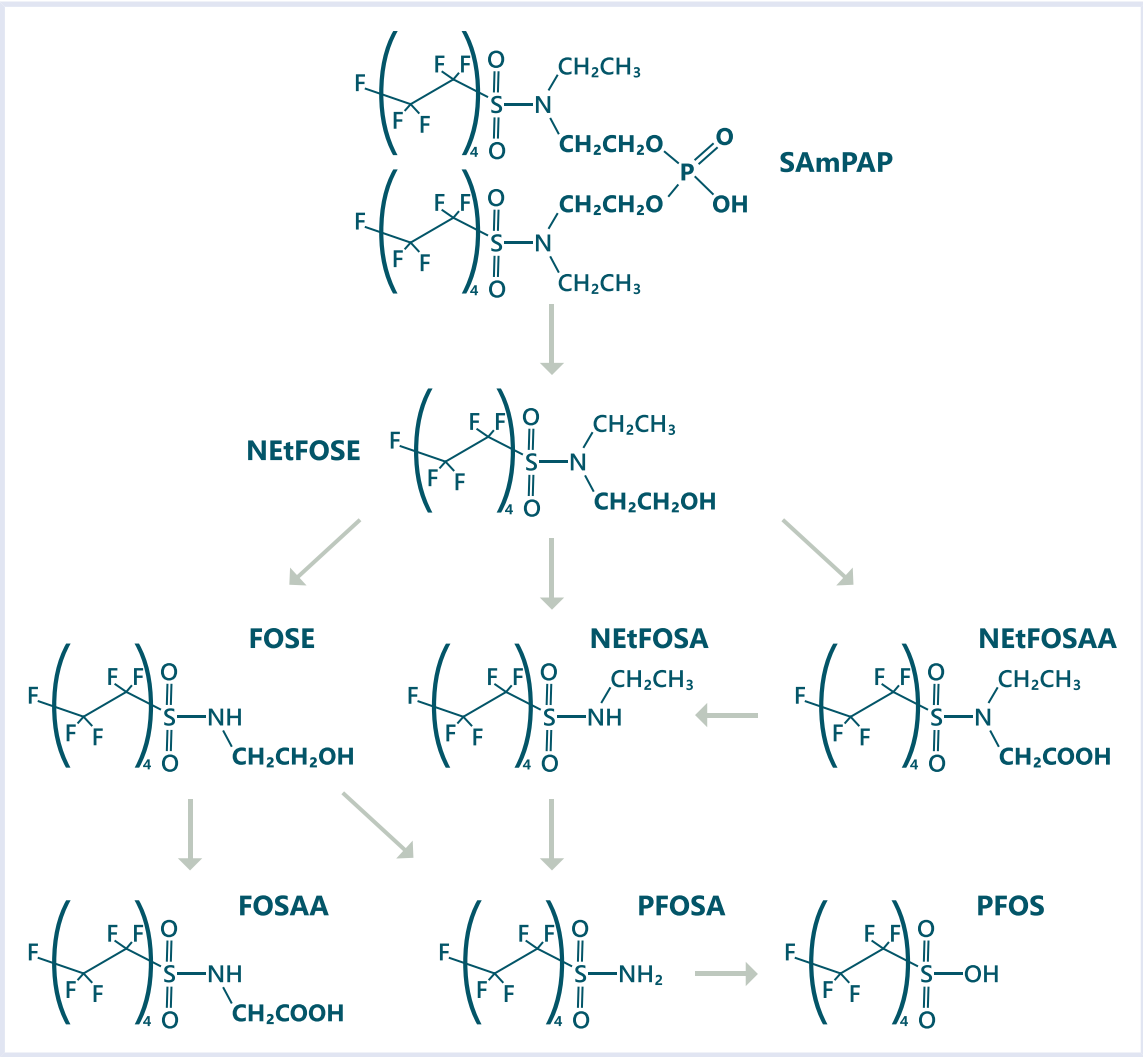

FIGURE 1 SAmPAP biotransformation processes in fish tissue, based on Peng et al. (2014) and Gaillard et al. (2017)

from 2.4 to 3.7 L/kg of organic carbon (ITRC, 2020b). For such chemicals, depuration from the sediment bed is rapid, and as a result, sediment remediation is unlikely to meaningfully reduce risks. However, some PFOS precursors (PreFOS; Martin et al., 2010) exhibit stronger partitioning. This complicates our understanding of the sources of PFOS in fish tissue and the pathways by which sediment- and water-column-borne precursors may contribute to tissue contamination.

Bioaccumulation modeling is often employed to investigate contaminant exposure sources and inform remedial action to reduce exposure. Early models addressed hydrophobic organic compounds (e.g., Arnot & Gobas, 2004; Connolly, 1991; Gobas et al., 1993; Thomann, 1989). Bioaccumulation models of ionic compounds have recently been developed (Armitage et al., 2013; Gobas et al., 2020; McDougall, 2016; Mittal & Ng, 2018; Ng & Hungerbühler, 2013; Vidal et al., 2019; see also Conder et al., 2021). Models have generally focused on single chemicals. A notable exception is the physiologically based pharmacokinetic (PBPK) model developed by Mittal and Ng (2018) that incorporates precursor biotransformation into PFOA.

This paper presents a bioaccumulation model of PFOS and selected precursors developed to evaluate the potential importance of contaminated food and water as sources of PFOS in aquatic organisms. The objective of this model is to help bridge the gap between risk assessment, PFOS bioaccumulation, and decision-making for contaminated sites. It simulates PFOS as well as multiple PreFOS in a cascade of biotransformations that terminate in PFOS in a prey fish and a predator fish, and includes exposure to both contaminated food and water and bioenergetics to quantitatively link growth, respiration, and consumption.

Specifically, this model represents an initial tool designed to explore the role of perfluorooctane sulfonamidoethanol-based phosphate diester (SAmPAP diester, hereafter referred to as SAmPAP) and its biotransformation products as

sources of PFOS to aquatic organisms (Figure 1). SAmPAP was a major component in paper coatings produced in the United States until it was phased out in 2002, although it is likely still produced in other countries (Benskin et al., 2012). It has been detected in marine sediment both at concentrations similar to that of PFOS (Benskin et al., 2012) and higher than PFOS (Langberg et al., 2020). SAmPAP is hydrophobic, with a LogK_{OW} (neutral form) value of 16 (Table S2-1), and its highly sorptive nature is indicated by measurements of sediment concentrations coincident with undetectable concentrations in porewater or surface water (Benskin et al., 2012; Langberg et al., 2020).

The transformation of SAmPAP leads to the production of PFOS as well as several intermediate compounds. Field samples have provided evidence of transformation of SAmPAP in freshwater and marine sediments (Benskin et al., 2012; Schaanning et al., 2020; Zhang et al., 2018). SAmPAP transformation products have been found in sediments, surface water, and aquatic organisms (Asher et al., 2012; Benskin et al., 2012; Franklin, 2016; Gebbink et al., 2016; Langberg et al., 2020; Martin et al., 2004, 2010; Schaanning et al., 2020; Sedlak et al., 2017; Simmonet-Laprade et al., 2019; Tomy et al., 2009). Some of the intermediates formed in the transformation of SAmPAP to PFOS were also commercially manufactured products and thus may have been discharged directly into the environment (Boulanger et al., 2005; Gilljam et al., 2016a, 2016b; Nascimento et al., 2018).

MODEL DEVELOPMENT

The model represents chemical uptake and loss across the gill, uptake from food and loss across the gut wall, growth dilution, and biotransformation. The model computes whole-body chemical concentrations. In general, the non-PFAS aspects of the model follow established modeling frameworks from the literature, for example articles by Arnot and Gobas (2004) and Connolly (1991), and are only briefly described herein. The PFAS aspects of the model are based on recent studies (e.g., Armitage et al., 2013; McDougall, 2016) or were developed for this effort and are described in more detail.

Equation (1) presents the overall mass balance. All other equations are presented in Table S1-1, and the parameters are defined in Table S1-2 (see Section S1 of the Supporting Information).

$$\frac{dM}{dt} = \left[k_1 C_w + k_D C_D\right] W - \left[k_2 + k_E + \sum_{i=1}^{n_{T1}} k_{M,i}\right] M + \sum_{i=1}^{n_{T2}} k_{M,i} M_i \quad (1)$$

where:

M = Mass of chemical in whole body (subscripted when referring to a chemical other than the one being computed; nanogram; ng)

C_W = Concentration of chemical in water (nanograms per liter; ng/L)

C_D = Concentration of chemical in diet (nanograms per gram in food; ng/g food)

W = Body weight (g wet weight)

k_1 = Chemical uptake rate from water (L/g wet weight-day)

k_D = Chemical uptake rate from food (g food/g wet weight-day)

k_2 = Rate constant for chemical loss across gills (1/day)

k_E = Fecal elimination rate constant (1/day)

$k_{M,i}$ = Rate constant of metabolic biotransformation from or to chemical I (1/day)

n_{T1}, n_{T2} = Number of metabolic biotransformations,

The first two terms represent uptake from water and food. Uptake from water is calculated as a gill ventilation rate multiplied by an efficiency of uptake (Equation S2). Ventilation rate is calculated from the respiration rate, dissolved oxygen concentration, and efficiency of oxygen uptake (Equation S3). Respiration rate is calculated as a function of body weight, temperature, and an activity coefficient (Equation S4).

Uptake from food is represented as a food consumption rate multiplied by an assimilation efficiency (Equation S5). Food consumption rate is calculated by summing the primary energetic costs incurred by the organism, respiration, and growth, and dividing by the food assimilation efficiency (Equation S6). The model calculates respiration, growth, and consumption on an energy basis, so the estimation of food consumption rate (grams [g] of food/g body weight-day) incorporates energy contents of the body, of oxygen, and of the food (Equation S6; Connolly, 1991). Growth dilution is incorporated into the chemical concentration-based version of Equation (1) and is calculated from the change in weight (parameter k_G; Equation S7).

Branchial uptake and elimination are modeled as a diffusive exchange process that depends on the gradient between the dissolved concentrations in ambient water and in blood. Branchial elimination was modeled using the approach of McDougall (2016), modified from Armitage et al. (2013) and Arnot and Gobas (2004), in which the gill uptake term is divided by a distribution coefficient that represents the ratio between whole-body concentration and concentration dissolved in water (D_{BW}; Equation S8). The gradient is thus calculated as the difference between the uptake term multiplied by ambient concentration and the elimination term multiplied by the whole-body concentration.

Fecal elimination is modeled as the product of feces production rate and a coefficient (K_{GB}) representing the relative concentration of each chemical in feces and whole body (Equation S9). The feces production rate is set equal to the food consumption rate multiplied by (1−A_D), where A_D = food assimilation efficiency.

The hypothesized in vivo biotransformation series for SAmPAP includes *N*-ethyl perfluorooctane sulfonamidoethanol (NEtFOSE), *N*-ethyl perfluorooctane sulfonamidoacetic acid (NEtFOSAA), perfluorooctane sulfonamidoethanol (FOSE), perfluorooctane sulfonamidoacetic acid

 DOI: 10.1002/ieam.4414

(FOSAA), *N*-ethyl perfluorooctane sulfonamide (NEtFOSA), perfluorooctanesulfonamide (PFOSA), and PFOS (Figure 1; after Peng et al., 2014 and Gaillard et al., 2017). Each biotransformation represented in Figure 1 is included in the model. Biotransformation rates are first order (Equations S1 and S10). The rates were determined by calibration to the Gaillard et al. (2017) and Peng et al. (2014) experiments. Following the allometric approach described by Arnot et al. (2009) and Nichols et al. (2013), biotransformation rates were scaled by body weight. Equation S10 presents this scaling using the rates calibrated to the Gaillard et al. (2017) experiment as the base rates ($k_{M0,i}$), for which fish weighing 60 g were used. The exponent γ_M was determined by calibration to the Peng et al. (2014) results.

Values for model parameters were estimated based on published information on PFAS toxicokinetics and bioenergetics, building on the results of previous modeling studies. Parameter values were then adjusted based on the results of three laboratory experiments in which fish were exposed to PFAS in food or water. All three experiments involved exposure and depuration periods. Martin et al. (2003a) exposed juvenile rainbow trout to PFOS in water. This experiment permitted refinement of parameters specifically related to PFOS toxicokinetics. Gaillard et al. (2017) exposed juvenile Eurasian perch to SAmPAP in food. The experiment included two groups of fish: "Test" fish were exposed to SAmPAP in food, and "control" fish were not fed contaminated food but were exposed to the same water as the test fish. This permitted evaluation of the role of biotransformation, elimination, and subsequent uptake from the water—a route that the experimental results indicated was significant and was included in the model. Peng et al. (2014) exposed juvenile Japanese medaka to SAmPAP in water. These latter two experiments permitted estimation of rates of uptake of SAmPAP from food and water and rates of biotransformation through a cascade of reactions ending in PFOS.

Details concerning the estimation of parameter values are presented in Section S1 of the Supporting Information. Conditions specific to the Gaillard et al. (2017) and Peng et al. (2014) experiments are described in Sections S3 and S4, respectively.

CALIBRATION

The model was calibrated in two steps. First, PFOS E_W, and D_{BW} values were adjusted to match the results of the experiments of Martin et al. (2003a). Next, a subset of other parameters (subject to the constraints discussed in the Model Development section) were modified to fit the model results to the data in both the Gaillard et al. (2017) and Peng et al. (2014) experiments. Model fit was judged qualitatively, prioritizing fit to PFOS, and then fit to the more abundant precursors. Additional discussion of model calibration is provided in Section S2 of the Supporting Information.

The overall fit of model results to the Gaillard et al. (2017) and Peng et al. (2014) experiments is represented in Figure 2 as model-data crossplots that include both experiments (including the Gaillard et al. [2017] test and control organisms) and all measured compounds, with different symbols for each chemical and different colors indicating model and data at the end of the exposure period

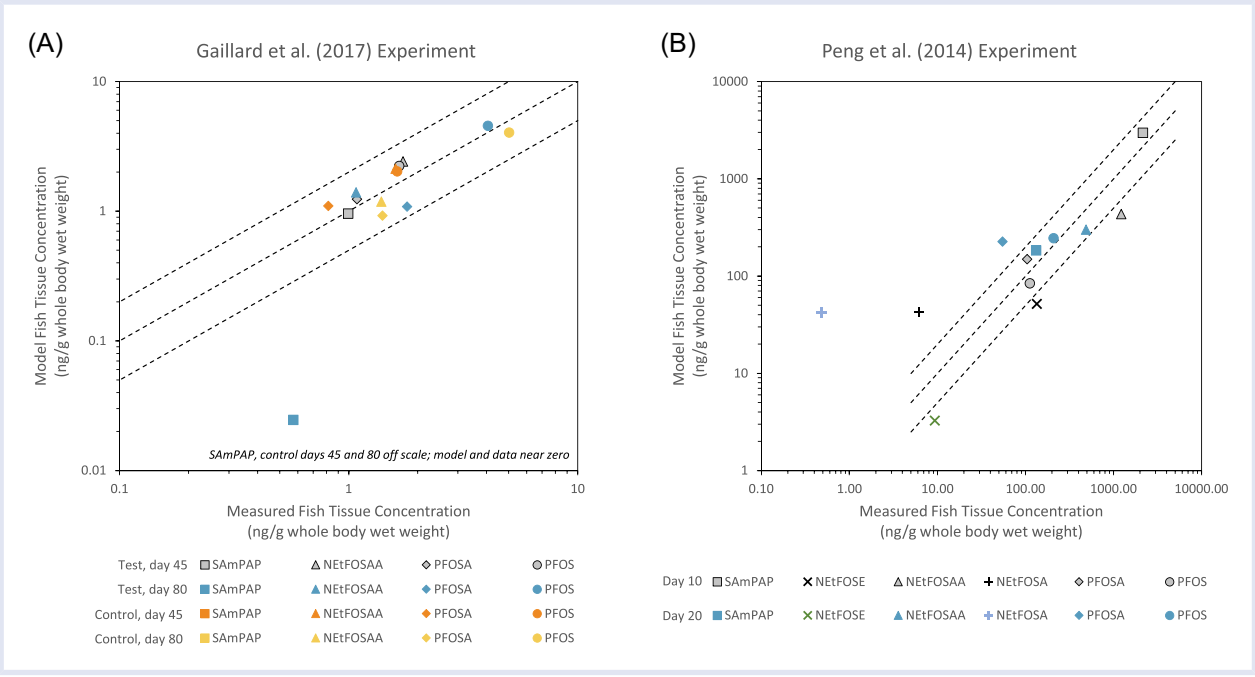

FIGURE 2 Modeled and laboratory-measured PreFOS and PFOS concentrations in fish exposed to SAmPAP. Concentrations at the end of the exposure and elimination periods. Values are provided in Table 1

TABLE 1 Modeled and laboratory-measured PreFOS and PFOS concentrations in fish exposed to SAmPAP

Study	Data/Model	Test/Control	Day	SAmPAP	NEtFOSE	NEtFOSAA	NEtFOSA	PFOSA	PFOS
Peng et al. (2014)	Data	–	10	2160.17	134.27	1220.20	6.26	104.40	112.06
	Model	–	20	2992.13	51.97	436.30	42.56	149.65	84.44
	Data	–	10	132.14	9.34	487.34	0.49	54.90	208.15
	Model	–	20	184.91	3.28	301.03	42.29	226.84	246.20
Gaillard et al. (2017)	Data	Test	45	1.00		1.73		1.09	1.66
	Model	Test	45	0.95		2.42		1.24	2.24
	Data	Control	45	0.06		1.60		0.82	1.63
	Model	Control	45	0.00		2.12		1.10	2.04
Gaillard et al. (2017)	Data	Test	80	0.57		1.08		1.80	4.06
	Model	Test	80	0.02		1.43		1.11	4.66
	Data	Control	80	0.00		1.39		1.41	5.03
	Model	Control	80	0.00		1.21		0.95	4.13

Abbreviations: NEtFOSA, *N*-ethyl perfluorooctane sulfonamide; NEtFOSAA, *N*-ethyl perfluorooctane sulfonamidoacetic acid; NEtFOSE, *N*-ethyl perfluorooctane sulfonamidoethanol; PFOS, perfluorooctane sulfonate; PFOSA, perfluorooctanesulfonamide; SAmPAP, perfluorooctane sulfonamidoethanol-based phosphate diester.

and at the end of the depuration period (see Table 1 for the values presented in Figure 2). For both experiments, modeled and measured concentrations are positively correlated and distributed around a line with log slope of one. Most modeled concentrations (and all PFOS concentrations) at the ends of the exposure periods and depuration periods lie within a factor of two of the data. Tissue concentrations for the Peng et al. (2014) experiment are two orders of magnitude higher than for the Gaillard et al. (2017) experiment because of differences in exposure (25 µg/L vs. 1631 ng/g) and differences in dietary vs. branchial uptake of SAmPAP. For the Peng et al. (2014) experiment, the compounds that are more than a factor of two off the 1:1 line are generally compounds present in smaller concentrations; thus, the model captures (within approximately a factor of 2) the compounds that are most abundant. Two values are not presented in this figure for SAmPAP in the Gaillard et al. (2017) experiment in the control fish on Days 45 and 80: Both model and data were very low on these days. Imprecision in estimating data values from figures in Gaillard et al. (2017) and uncertainties associated with the possible presence of small amounts of dissolved SAmPAP in the experimental tanks contributed to differences between the model and data at these very low concentrations.

The modeled PFOS time courses qualitatively capture the patterns in the data. In both experiments, including the Gaillard et al. (2017) test and control fish, modeled and measured PFOS (Figure 3) increases throughout both the exposure and the depuration periods. In the Gaillard et al. (2017) experiment, the test fish time course is well represented; a small increase in initial background concentration (initial concentrations in the model reported by the authors) would improve the fit early in the simulation. The control fish rise within approximately 10% of the single measured value. The model does not capture all of the short-term dynamics; in the Peng et al. (2014) experiment, the data indicate a more rapid increase early in the experiment than is computed by the model.

Additional calibration discussion is provided in Section S7 of the Supporting Information.

MODEL EVALUATION

Bioconcentration factors

Fish whole-body and carcass PFOS bioconcentration factors (BCFs) were measured in the laboratory by Inoue et al. (2012) and Sakurai et al. (2013); see Section S5 of the Supporting Information. When the conditions of these experiments were matched based on the information provided in the publications, the model yielded BCFs of 950 for both studies, which lies within 10% of the measured values: 1000 (Inoue et al., 2012) and 910 (Sakurai et al., 2013). These values were also similar to the BCF measured by Martin et al. (2003a): 1100 L/kg whole-body wet weight. For two other studies (see Section S5), the model underpredicted the BCF: Fangfang (2014) measured 2400, and the model calculated 810; and Wildlife International (2002) measured 2800, and the model calculated 950. However, compared with the other three studies, less information was provided regarding the experimental conditions for these two studies, so these comparisons are less certain.

Biomagnification factors

Modeled whole-body PFOS biomagnification factors (BMFs) based on water and food exposure were greater than for food-only. Values ranging from 1 to 2 were

 DOI: 10.1002/ieam.4414

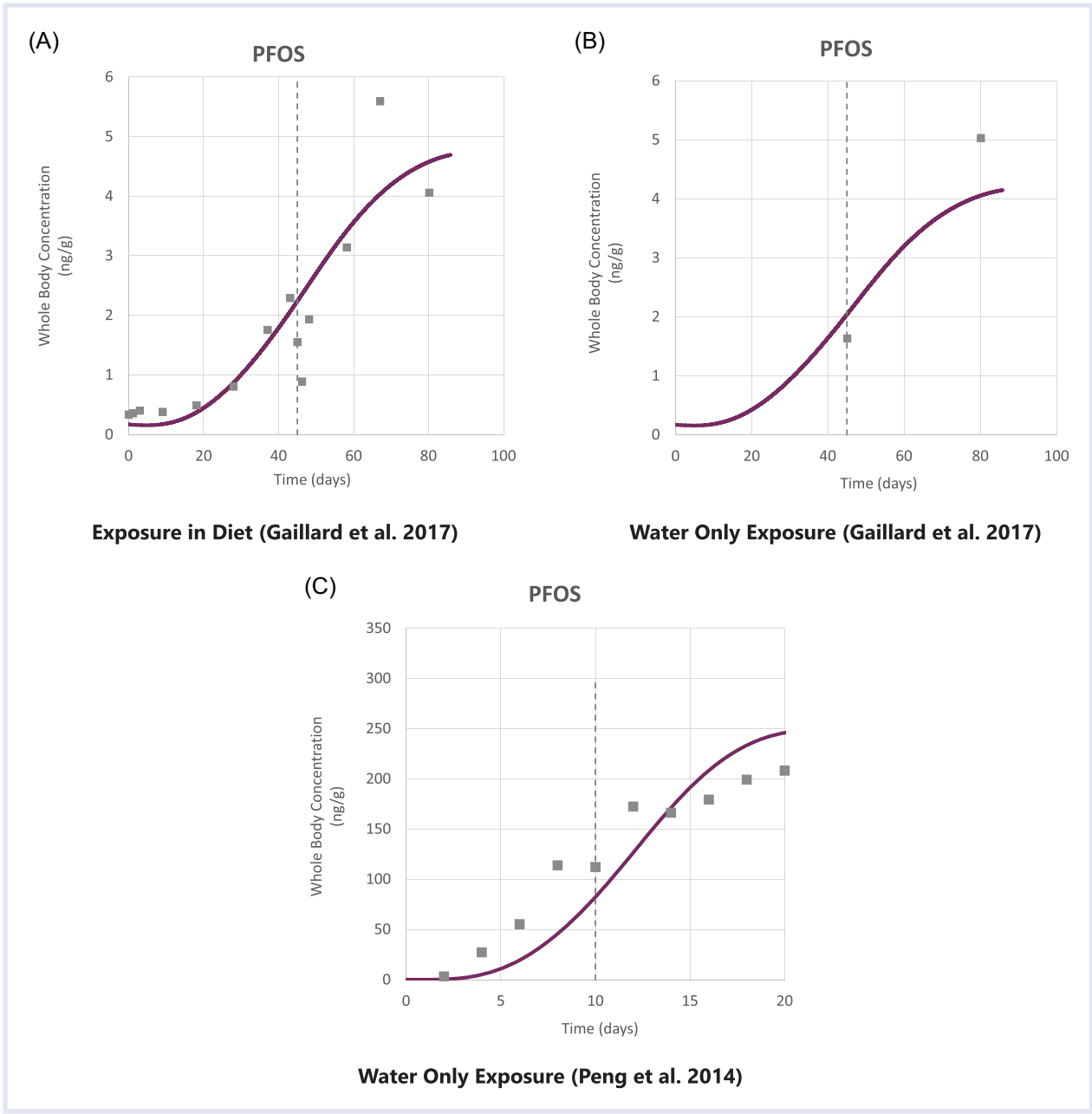

FIGURE 3 Time courses of modeled and laboratory-measured PFOS concentrations in fish exposed to SAmPAP. (A) Gaillard et al. (2017), exposure to SAmPAP in diet. (B) Gaillard et al. (2017), exposure to PreFOS in water only. (C) Peng et al. (2014), exposure to SAmPAP in water only

computed for predator fish exposed to PFOS only in their prey (body weight 100–1000 g, respiration coefficient beta 0.1–0.2 kJ/g wet weight-day). Values ranging from 2 to 3 were computed for prey and predator fish exposed to PFOS in water and in both food and water.

Modeled whole-body PFOS BMF values for predator fish exposed to SAmPAP in food or to NEtFOSE in water ranged from 2 to 8. These two scenarios were selected to provide example results for two different PreFOS in two media. The BMFs were higher than in the PFOS-only exposures because some of the original SAmPAP or NEtFOSE to which the prey were exposed remained in the tissues of the prey and was biotransformed by the predator into PFOS.

The BMF values computed by the model, both with and without PreFOS, lie within the range of measured BMFs (Section S6). Field-measured PFOS BMF values range from 0.4 to 31 (g whole-body wet weight/g whole-body wet weight; only including studies in which the compared species are reasonably temporally and spatially matched and are considered to be within the same food web [e.g., benthic vs. pelagic]; values provided in Table S6-1 of the Supporting Information; the Langberg et al. [2020] study was not included because of the clear evidence of a strong influence of PreFOS). The median of the 62 compiled values is 2.0; the arithmetic average is 4.0 ± 5.4 (SD). Approximately 80% of the values lie between 1 and 10. BMFs are

uncertain because they condense complex diets to a simple pairing of a predator with a single prey item, often with a variable difference in trophic levels. Therefore, modeled BMFs were also compared with trophic magnification factors (TMFs) reported by the same authors. TMFs have the advantage of incorporating multiple species in a range of trophic levels as well as potentially more refined estimates of trophic position using del^{15}N. The distribution of data-based TMFs is similar to the measured BMFs (Table S6-2): The median of 11 values is 2.5 and the average 3.1, with values ranging from 0.94 to 6.3.

Model testing could be refined further by accounting for the fact that the field-measured PFOS BMF and TMF values may be inflated owing to the presence of PreFOS. Langberg et al. (2020) measured TMFs and BAFs in a food web strongly impacted by high concentrations of SAmPAP in sediments. PFOS TMFs ranged from 4 to 9 in perch muscle, similar to the range of values computed by the model for SAmPAP exposure. This similarity supports the realism of the model, although only semi-quantitatively, acknowledging that the details of the diets and bioenergetics of the modeled and sampled fish may be different. PreFOS were measured in four of the remaining studies (and not reported in the fifth, although they likely were present; see Table S6-2 of the Supporting Information). Such refinements at this point would be partial because the PreFOS measured in the available field studies represent only a subset of all potential PreFOS.

Uncertainty

Using parameter values that honor the available experimental studies, the model presented here yields results that compare favorably with concentrations of several chemicals measured in two separate experiments with differing exposure sources. However, consistency with the experimental measurements does not tightly constrain some model parameters. For most PreFOS, the results are not very sensitive to the parameters that control uptake and loss of the intermediate PreFOS (E_D, E_W, D_{BW}, and K_{GB}), and thus calibration does not yield highly certain values for these parameters. This is because intentional exposure was limited to SAmPAP and loss rates are controlled by the rates of biotransformation. Uncertainty in uptake parameters potentially limits the applicability of the model in situations in which intermediate PreFOS are significant exposure sources. In addition, uncertainty in parameters affecting loss rates would be potentially important for organisms with low rates of biotransformation. Additional laboratory measurements of these rates would further constrain these model parameters, improve model reliability, and widen its applicability.

MODEL APPLICATIONS

Impact of PreFOS on PFOS concentrations in biota and bioaccumulation metrics

The variability in field-measured PFOS BMFs and TMFs is caused by multiple factors, including variation in growth rates, age, and bioenergetics; uncertainties in diet; non-steady-state conditions; and the presence of PreFOS (e.g., Franklin, 2016). A comparison of the range of BMFs computed by the model (2–8), across several scenarios involving two PreFOS, against the range of field-measured BAFs (0.4–31) suggests that the presence of PreFOS may account for a portion of the observed variability in field-measured PFOS BMFs but not all. This conclusion is preliminary, however, because all possible PFOS precursors have not been identified or modeled.

To further explore the impacts of individual PreFOS on the measured PFOS BMF, a series of model simulations was performed including exposure to PFOS in the water at 1 ng/L along with one PreFOS. SAmPAP was added to the food in one set of simulations, NEtFOSAA was added to water in a second set, and PFOSA was added to water in a third. The computed whole-body PFOS predator–prey BMFs are presented in Figure 4 as a function of the concentration of each PreFOS in food or water. The apparent PFOS BMF (i.e., the predator–prey PFOS concentration ratio) rises to a maximum level at elevated PreFOS concentrations and does not increase beyond this value as PreFOS concentrations continue to increase. The impact of PreFOS on the PFOS BMF depends on the particular PreFOS. With NEtFOSAA exposure, the PFOS BMF rises from 2.6 (PFOS in water-only) to a maximum of approximately 5. This represents a realistic environmental condition: Benskin et al. (2012) measured a NEtFOSAA concentration in water of approximately 60 ng/L, which produces a BMF of approximately 5. SAmPAP exposure in food produces somewhat less of an impact on the PFOS BMF, ranging up to approximately 4. BMF values as high as 4 are realistic for such a scenario, based on the PFOS and SAmPAP concentrations measured by Langberg et al. (2020; maximum sediment SAmPAP concentration of 1900 ng/g, PFOS concentration in water approximately 0.3 ng/L,

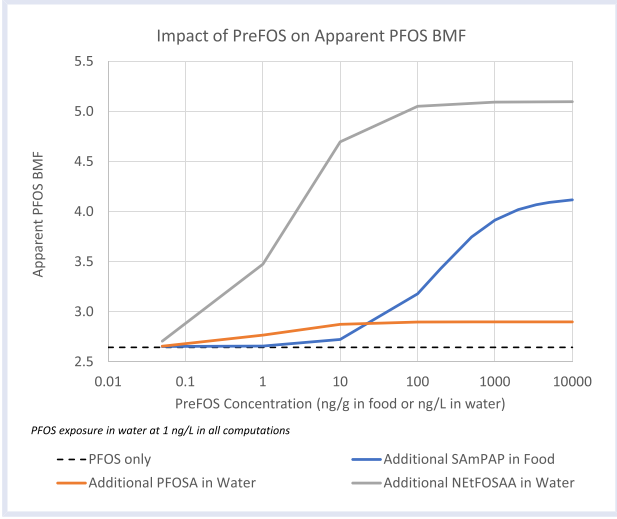

FIGURE 4 Impact of exposure to individual PreFOS on the apparent PFOS BMF. Model simulations performed including 1 ng/L PFOS plus individual PreFOS at a range of concentrations

 DOI: 10.1002/ieam.4414

producing a BMF of approximately 4). Finally, PFOSA in water has a smaller effect, increasing the PFOS BMF to approximately 3 at higher PFOSA concentrations, which is an increase of a few percent. This is because most of the PFOSA is transformed in the prey tissues, so the exposure of the predator is primarily to PFOS in prey and little additional biotransformation occurs in the predator. Thus, the measured PFOS BMF varies with the particular combination of PreFOS present in the environment.

PreFOS exposure is likely to affect BAFs to a much greater degree than BMFs or TMFs. The PFOS BAF values measured by Langberg et al. (2020) ranged up to 250 000 in muscle—one to two orders of magnitude higher than published studies (e.g., Asher et al., 2012; Gebbink et al., 2016; Houde et al., 2008; Khairy et al., 2019)—whereas the BMFs measured by Langberg et al. (2020) and computed by the model (with PreFOS exposure) were within the range of values measured at various sites and only two to three times higher than the median of the observed BMFs and the modeled PFOS-only BMFs. These patterns are understandable given the exposure conditions in the Langberg et al. (2020) study and the process of biotransformation: With predominant exposure to PreFOS in the environment, the measured PFOS BAF is high because the denominator in the equation (i.e., the PFOS aqueous concentration) is low, whereas the numerator (PFOS in tissues) is elevated owing to biotransformation of the PreFOS that are taken up. The impact of PreFOS on PFOS BMFs is more limited: Because prey organisms likely transform a portion of PreFOS in their diet to PFOS within their tissues, predators are exposed to a significant amount of PFOS in their diet (although the ultimate exposure of the prey is only to PreFOS). Thus, the measured PFOS BMFs do not vary as much as measured BAFs in the presence of significant exposure to PreFOS.

Impact of PreFOS on response time

Tissue concentrations respond within weeks to changes in exposure to PFOS and PreFOS (e.g., Martin et al., 2003a; Gaillard et al., 2017; Peng et al., 2014). Response times are more rapid than other organic compounds such as higher chlorinated polychlorinated biphenyls (PCBs), in part because PFOS is eliminated rapidly and in part because many of the calibrated rates of PreFOS biotransformation are faster than gill and fecal elimination and growth dilution. To explore this further, model simulations were performed with prey and predator experiencing short-term exposure to PFAS in their food or water. After exposure to PFOS in water for 10 days, prey and predator concentrations rise and then fall, declining to 5% of the maximum concentration achieved during the exposure period within 190 and 430 days of achieving that maximum concentration, respectively. The predator response time is longer because its exposure continues after the concentrations in sediments and water have returned to low values, owing to residual contamination in the prey.

Exposure to PreFOS lengthens the response time. For example, after exposure for 10 days to NEtFOSAA in water, concentrations rise and then decline to 5% of their maximum concentration within 280 and 500 days of achieving the maximum concentration. After exposure for 10 days to SAmPAP in food, concentrations rise and then decline to 5% of their maximum concentration within 330 and 590 days of achieving the maximum concentration. Based on these examples, it is expected that, in the field, concentrations in fish tissue generally will respond to changes in exposure within 1–2 years, and the presence of PreFOS will delay the response. It is noted that concentrations in air-breathing organisms may respond more slowly, depending on their biotransformation rates as well as the fact that depuration associated with air exchange is slower than for gill-breathing organisms.

Role of SAmPAP as a source of PFOS in tissue

Setting concentrations in the food of the prey fish equal to concentrations of SAmPAP that have been measured in the environment (approximately 0.2 ng/g; Benskin et al., 2012; Zhang et al., 2018), computed PFOS concentrations are much lower than tissue concentrations that are of concern in fish consumption advisories. For example, the relatively restrictive draft fish consumption advisory from New Jersey includes 0.56 ng/g in fillets as the target PFOS concentration for unlimited consumption. The ratio of muscle to whole-body PFOS concentrations ranges from approximately 0.5 to 1.0 (Goeritz et al., 2013; Shi et al., 2015). The predicted whole-body concentrations for a SAmPAP exposure concentration of 0.2 ng/g in the food of the prey fish (0.00088 and 0.0037, respectively) are two to three orders of magnitude lower than the fish advisory level (values are similarly low for a range of respiration rates and body weights). A source of uncertainty with this conclusion is the amount of bioaccumulation that occurs at the base of the food web. Unless concentrations in the invertebrate food of the prey fish are orders of magnitude greater than concentrations in sediments on which they may feed, this result can be extrapolated qualitatively to SAmPAP in sediments: At these concentrations, ingested SAmPAP is unlikely to account for PFOS concentrations in tissue that approach advisory limits.

In contrast, if the exposure concentrations in the food of the prey are set equal to the concentrations of SAmPAP measured in sediments by Langberg et al. (2020), approximately 500 ng/g, then the computed whole-body tissue concentrations in prey and predator, 2 and 9 ng/g, respectively (for 100 g prey and 1000 g predator), are within the range of state advisory levels (e.g., the New Jersey weekly consumption trigger = 3.9 ng/g). Under such conditions, existing PreFOS concentrations in sediments are sufficient to lead to PFOS concentrations in fish tissue that are potentially of regulatory concern.

Because SAmPAP partitions strongly to sediments, it is expected to be persistent in the environment. Transformation of SAmPAP in the environment, to the extent that it occurs, would reduce its persistence. The evidence of transformation in the environment is mixed: In the

laboratory, Benskin et al. (2013) found negligible loss over the course of 120 days in marine sediments, whereas Zhang et al. (2018) found a half-life of 88 days in freshwater sediments. Transformation in the environment into more bioavailable PreFOS, to the extent it occurs, would likely increase the accumulation of PFOS in aquatic organisms because SAmPAP appears to be taken up from water and sediment with lower efficiency than other PreFOS. But SAmPAP transformation would also reduce its persistence. Characterization of SAmPAP transformation in sediments and water and of the impacts of environmental transformation on persistence and bioaccumulation are critical to effectively managing PFOS levels in aquatic organisms. There is thus a need for more information regarding rates of transformation in the environment.

NEXT STEPS

The model presented here highlights areas of uncertainty that would benefit from additional research. Because the model focuses on the biotransformation cascade originating in SAmPAP, its calibration to the laboratory experiments was not sensitive to the uptake kinetics of the other PreFOS. Several of the PreFOS in the SAmPAP cascade have likely been discharged themselves and have been found in the environment. Therefore, experimental and modeling work to understand their uptake kinetics is needed. Similarly, study of the biotransformation and toxicokinetics of other PreFOS in the environment (e.g., compounds found in AFFF) is a logical next step.

Biotransformation rates generally exceed PreFOS branchial and fecal loss rates and thus likely control PreFOS concentrations and the PFOS production rate to a large degree. This means that estimating all fecal and branchial elimination rates for all PreFOS in fish is probably not critical to developing an understanding of PFOS sources. However, there is room for refinement of biotransformation pathways and rates, because the model does not match the time courses of all individual chemicals in the two experiments (e.g., PFOSA). Refinement of the biotransformation rates may affect the relative abundance of PreFOS in fish tissue, which may be useful in evaluating PFAS sources.

Models such as the one presented here can support the evaluation of the sources of PFOS in aquatic organisms and thus support remedial decision-making, combining realistic PFOS and PreFOS toxicokinetics and bioenergetics in a framework that includes both food and water exposure, as well as predator–prey relationships. At its current stage of development, the model can provide useful insights regarding source evaluation and the potential impacts of alternative remedial plans at specific sites, thus providing one line of evidence in support of decision-making. As new field and laboratory data become available, supporting greater understanding of the identity of all potential PreFOS (as well as their uptake, loss, and biotransformation), the model's usefulness as a decision-support tool will increase.

One metric of potential use in evaluating remedial options is the ratio of PreFOS–PFOS concentrations throughout the food web. More detailed studies of the relative concentrations of the various PreFOS compounds in tissue will also be informative. Sampling organisms at lower trophic levels is likely to be more useful than organisms at upper trophic levels because the PreFOS compounds are likely to be in larger proportion. Models such as the one presented here will aid in interpreting field measurements and in identifying PFOS sources to aquatic food webs, thus supporting decision making regarding the reduction in ecological and human health risks associated with PFAS.

ACKNOWLEDGMENT

This research was funded by Anchor QEA, LLC. We acknowledge Betsy Henry of Anchor QEA for a helpful review.

CONFLICT OF INTEREST

The authors declare that there are no conflict of interests.

DATA AVAILABILITY STATEMENT

The data used in model development are available from corresponding author David Glaser upon request (dglaser@anchorqea.com).

SUPPORTING INFORMATION

Figure S7-1. Modeled and laboratory-measured concentrations of SAmPAP and transformation products in fish exposed to SAmPAP (exposure in diet [Gaillard et al. 2017]).

Figure S7-2. Modeled and laboratory-measured concentrations of SAmPAP and transformation products in fish exposed to SAmPAP (water-only exposure [Gaillard et al. 2017]).

Figure S7-3. Modeled and laboratory-measured concentrations of SAmPAP and transformation products in fish exposed to SAmPAP (water-only exposure [Peng et al. 2014]).

Table S1-1. Model equations.

Table S1-2. Model variables and parameters.

Table S1-3. Chemical-specific model parameter values.

Table S2-1. Physical/chemical parameters.

Table S2-2. Whole-body composition

Table S2-3. Calculation of D_{BW}.

Table S5-1. BCF experiments: Study-specific conditions and measured and modeled BCFs.

Table S6-1. PFOS biomagnification factors.

Table S6-2. PFOS trophic magnification factors.

Table S7-1. PFOS loss rates computed by the model.

REFERENCES

Armitage, J. M., Arnot, J. A., Wania, F., & Mackay, D. (2013). Development and evaluation of a mechanistic bioconcentration model for ionogenic organic chemicals in fish. *Environmental Toxicology and Chemistry*, *32*(1), 115–128.

Arnot, J. A., & Gobas, F. A. P. C. (2004). A food web bioaccumulation model for organic chemicals in aquatic ecosystems. *Environmental Toxicology and Chemistry*, *23*(10), 2343–2355.

Arnot, J. A., Meylan, W., Tunkel, J., Howard, P. H., Mackay, D., Bonnell, M., & Boethling, R. S. (2009). A quantitative structure-activity relationship for

predicting metabolic biotransformation rates for organic chemicals in fish. *Environmental Toxicology and Chemistry*, *28*, 1168–1177.

Asher, B. J., Wang, Y., De Silva, A. O., Backus, S., Muir, D. C. G., Wong, C. S., & Martin, J. W. (2012). Enantiospecific perfluorooctane sulfonate (PFOS) analysis reveals evidence for the source contribution of PFOS-precursors to the Lake Ontario foodweb. *Environmental Science and Technology*, *46*, 7653–7660.

Benskin, J. P., Ikonomou, M. G., Gobas, F. A. P. C., Begley, T. H., Woudneh, M. B., & Cosgrove, J. R. (2013). Biodegradation of *N*-ethyl perfluorooctane sulfonamido ethanol (EtFOSE) and EtFOSE-based phosphate diester (SAmPAP diester) in marine sediments. *Environmental Science and Technology*, *47*, 1381–1389.

Benskin, J. P., Ikonomou, M. G., Gobas, F. A. P. C., Woudneh, M. N., & Cosgrove, J. R. (2012). Observation of a novel PFOS-precursor, the perfluorooctane sulfonamido ethanol-based phosphate (SAmPAP) diester, in marine sediments. *Environmental Science and Technology*, *46*, 6505–6514.

Boisvert, G., Sonne, C., Rigét, F. F., Dietz, R., & Letcher, R. J. (2019). Bioaccumulation and biomagnification of perfluoroalkyl acids and precursors in East Greenland polar bears and their ringed seal prey. *Environmental Pollution*, *252*, 1335–1343.

Boulanger, B., Vargo, J. D., Schnoor, J. L., & Hornbuckle, K. C. (2005). Evaluation of perfluorooctane surfactants in a wastewater treatment system and in a commercial surface protection product. *Environmental Science and Technology*, *39*, 5524–5530.

Conder, J., Zodrow, J., Arblaster, J., Kelly, B., Gobas, F., Suski, J., Osborn, E., Frenchmeyer, M., Divine, C., & Leeson, A. (2021). Strategic resources for assessing PFAS ecological risks at AFFF sites. *Integrated Environmental Assessment and Management*, *17*(4), 746–752.

Connolly, J. P. (1991). Application of a food chain model to polychlorinated biphenyl contamination of the lobster and winter flounder food chains in New Bedford Harbor. *Environmental Science and Technology*, *25*, 760–770.

European Union (EU). (2013). Directive 2013/39/EU of the European Parliament and of the Council of 12 August 2013 Amending Directives 2000/60/EC and 2008/105/EC as regards priority substances in the field of water policy (Text with EPA Relevance). *Official Journal of the European Union*, (*226*), 1–17.

Fangfang, C. (2014). *Bioaccumulation, tissue distribution and maternal transfer of ionogenic organic contaminants in zebrafish (Danio rerio)* (Doctorate thesis, National University of Singapore, NUS Graduate School for Integrative Sciences and Engineering, Singapore).

Franklin, J. (2016). How reliable are field-derived biomagnification factors and trophic magnification factors as indicators of bioaccumulation potential? Conclusions from a case study on per- and polyfluoroalkyl substances. *Integrated Environmental Assessment and Management*, *12*(1), 6–20.

Gaillard, J., Veyrand, B., Thomas, M., Dauchy, X., Boiteux, V., Marchand, P., Le Bizec, B., Banas, D., & Feidt, C. (2017). Tissue uptake, distribution, and elimination of perfluoroalkyl substances in juvenile perch through perfluorooctane sulfonamidoethanol based phosphate diester dietary exposure. *Environmental Science and Technology*, *51*, 7658–7666.

Gebbink, W. A., Bignert, A., & Berger, U. (2016). Perfluoroalkyl acids (PFAAs) and selected precursors in the Baltic Sea environment: Do precursors play a role in food web accumulation of PFAAs? *Environmental Science and Technology*, *50*, 6354–6362.

Gilljam, J. L., Leonel, J., Cousins, I. T., & Benskin, J. P. (2016a). Is ongoing sulfluramid use in South America a significant source of perfluorooctanesulfonate (PFOS)? Production inventories, environmental fate, and local occurrence. *Environmental Science and Technology*, *50*, 653–659.

Gilljam, J. L., Leonel, J., Cousins, I. T., & Benskin, J. P. (2016b). Additions and correction to "Is ongoing sulfluramid use in South America a significant source of perfluorooctanesulfonate (PFOS)? Production inventories, environmental fate, and local occurrence". *Environmental Science and Technology*, *50*, 7930–7933.

Gobas, F. A. P. C., Kelly, B. C., & Kim, J. J. (2020). *A framework for assessing bioaccumulation and exposure risks of per and polyfluoroalkyl substances in threatened and endangered species on aqueous film forming foam (AFFF)-impacted sites*. Project ER18-1502. Alexandria, VA: Department of Defense Strategic Environmental Research and Development Program (SERDP).

Gobas, F. A. P. C., Zheng, X., & Wells, R. (1993). Gastrointestinal magnification: The mechanism of biomagnification and food chain accumulation of organic chemicals. *Environmental Science and Technology*, *27*, 2855–2863.

Goeritz, I., Falk, S., Stahl, T., Schäfers, C., & Schlechtriem, C. (2013). Biomagnification and tissue distribution of perfluoroalkyl substances (PFASs) in market-size rainbow trout (*Oncorhynchus mykiss*). *Environmental Toxicology and Chemistry*, *32*(9), 2078–2088.

Houde, M., Czub, G., Small, J. M., Backus, S., Wang, X., Alaee, M., & Muir, D. C. G. (2008). Fractionation and bioaccumulation of perfluorooctane sulfonate (PFOS) isomers in a Lake Ontario food web. *Environmental Science and Technology*, *42*, 9397–9403.

Inoue, Y., Hashizume, N., Yakata, N., Murakami, H., Suzuki, Y., Kikushima, E., & Otsuka, M. (2012). Unique physiochemical properties of perfluorinated compounds and their bioconcentration in common carp *Cyprinus carpio* L. *Archives of Environmental Contamination and Toxicology*, *62*, 672–680.

Interstate Technology Regulatory Council (ITRC). (2020a). *Regulations, guidance, and advisories for per- and polyfluoroalkyl substances (PFAS)*. ITRC, PFAS Team.

Interstate Technology Regulatory Council (ITRC). (2020b). Environmental fate and transport for per- and polyfluoroalkyl substances. ITRC, PFAS Team.

Khairy, M. A., Noona, G. O., & Lohmann, R. (2019). Uptake of hydrophobic organic compounds, including organochlorine pesticides, polybrominated diphenyl ethers, and perfluoroalkyl acids in fish and blue crabs of the Lower Passaic River, New Jersey, USA. *Environmental Toxicology and Chemistry*, *38*(4), 872–882.

Langberg, H. A., Breedveld, G. D., Slinde, G. A., Grønning, H. M., Høisæter, A., Jartun, M., Rundberget, T., Jenssen, B. M., & Hale, S. E. (2020). Fluorinated precursor compounds in sediments as a source of perfluorinated alkyl acids (PFAA) to biota. *Environmental Science and Technology*, *54*, 13077–13089.

Martin, J. W., Asher, B. J., Beesoon, S., Benskin, J. P., & Ross, M. S. (2010). PFOS or PreFOS? Are perfluorooctane sulfonate precursors (PreFOS) important determinants of human and environmental perfluorooctane sulfonate (PFOS) exposure? *Journal of Environmental Monitoring*, *12*(11), 1929–2188.

Martin, J. W., Mabury, S. A., Solomon, K. R., & Muir, D. C. G. (2003a). Bioconcentration and tissue distribution of perfluorinated acids in rainbow trout (*Oncorhynchus mykiss*). *Environmental Toxicology and Chemistry*, *22*(1), 196–204.

Martin, J. W., Mabury, S. A., Solomon, K. R., & Muir, D. C. G. (2003b). Dietary accumulation of perfluorinated acids in juvenile rainbow trout (*Oncorhynchus mykiss*). *Environmental Toxicology and Chemistry*, *22*(1), 189–195.

Martin, J. W., Whittle, D. M., Muir, D. C. G., & Mabury, S. A. (2004). Perfluoroalkyl contaminants in a food web from Lake Ontario. *Environmental Science and Technology*, *38*, 5379–5385.

McDougall, M. R. R. (2016). *Developing a trophic bioaccumulation model for PFOA and PFOS in a marine food web* (Master's thesis). Burnaby, BC, Canada: Simon Fraser University, School of Resource and Environment Management.

Minnesota Department of Health (MDH). (2018). *Fish consumption guidelines for women who are or may become pregnant, and children under age 15, lakes*. https://www.health.state.mn.us/communities/environment/fish/docs/eating/specpoplakes.pdf

Mittal, V. K., & Ng, C. A. (2018). Formation of PFAAs in fish through biotransformation: A PBPK approach. *Chemosphere*, *202*, 218–227.

Nascimento, R. A., Nunoo, D. B. O., Bizkarguenaga, E., Schultes, L., Zabaleta, I., Benskin, J. P., Spanó, S., & Leonel, J. (2018). Sulfluramid use in Brazilian agriculture: A source of per- and polyfluoroalkyl substances (PFASs) to the environment. *Environmental Pollution*, *242*, 1436–1443.

Ng, C. A., & Hungerbühler, K. (2013). Bioconcentration of perfluorinated alkyl acids: How important is specific binding? *Environmental Science and Technology*, *47*, 7214–7223.

Nichols, J. W., Huggett, D. B., Arnot, J. A., Fitzsimmons, P. N., & Cowan-Ellsberry, C. E. (2013). Toward improved models for predicting bioconcentration of well-metabolized compounds by rainbow trout using measured rates of in vitro intrinsic clearance. *Environmental Toxicology and Chemistry*, *32*(7), 1611–1622.

Organisation for Economic Co-Operation and Development (OECD). (2018). *Toward a new comprehensive global database of per- and polyfluoroalkyl substances (PFASs): Summary report on updating the OECD 2007 list of per- and polyfluoroalkyl substances (PFASs)*. Series on Risk Management No. 39. ENV/JM/MONO(2018)7. OECD Environment Directorate.

Peng, H., Zhang, H., Sun, J., Zhang, Z., Giesy, J. P., & Hu, J. (2014). Isomer-specific accumulation of perfluorooctanesulfonate from (*N*-ethyl perfluorooctanesulfonamido)ethanol-based phosphate diester in Japanese medaka (*Oryzias latipes*). *Environmental Science and Technology*, *48*, 1058–1066.

Sakurai, T., Kobayashi, J., Kinoshita, K., Ito, N., Serizawa, S., Shiraishi, H., Lee, J., Horiguchi, T., Maki, H., Mizukawa, K., Imaizumi, Y., Kawai, T., & Suzuki, N. (2013). Transfer kinetics of perfluorooctane sulfonate from water and sediment to a marine benthic fish, the marbled flounder (*Pseudopleuronectes yokohamae*). *Environmental Toxicology and Chemistry*, *32*(9), 2009–2017.

Schaanning, M. T., Rundberget, J. T., & Jenssen, M. T. S. (2020). *Bioavailability and bioaccumulation of perfluorinated compounds (PFAS) in a polluted river sediment* (Report SNO 7472-2020. 26). Norwegian Institute for Water Research.

Sedlak, M. D., Benskin, J. P., Wong, A., Grace, R., & Greig, D. J. (2017). Per- and polyfluoroalkyl substances (PFASs) in San Francisco Bay wildlife: Temporal trends, exposure pathways, and notable presence of precursor compounds. *Chemosphere*, *185*, 1217–1226.

Shi, Y., Vestergren, R., Zhou, Z., Song, X., Xu, L., Liang, Y., & Cai, Y. (2015). Tissue distribution and whole body burden of the chlorinated polyfluoroalkyl ether sulfonic acid F-53B in crucian carp (*Carassius carassius*): Evidence for a highly bioaccumulative contaminant of emerging concern. *Environmental Science and Technology*, *49*, 14156–14165.

Simmonet-Laprade, C., Budzinski, H., Maciejewski, K., Le Manach, K., Santos, R., Alliot, F., Goutte, A., & Labadie, P. (2019). Biomagnification of perfluoroalkyl acids (PFAAs) in the food web of an urban river: Assessment of the trophic transfer of targeted and unknown precursors and implications. *Environmental Science: Processes and Impacts*, *21*, 1864–1874.

Thomann, R. V. (1989). Bioaccumulation model of organic chemical distribution in aquatic food chains. *Environmental Science and Technology*, *23*, 699–707.

Tomy, G. T., Pleskach, K., Ferguson, S. H., Hare, J., Stern, G., Macinnis, G., Marvin, C. H., & Loseto, L. (2009). Trophodynamics of some PFCs and BFRs in a western Canadian arctic marine food web. *Environmental Science and Technology*, *43*, 4076–4081.

Vidal, A., Babut, M., Garric, J., & Beaudouin, R. (2019). Elucidating the fate of perfluorooctanoate sulfonate using a rainbow trout (*Oncorhynchus mykiss*) physiologically-based toxicokinetic model. *Science of the Total Environment*, *691*, 1297–1309.

Wildlife International. (2002). Bioconcentration revised test substance: Perfluorooctanesulfonate. AR226_1108. Wildlife International.

Zhang, S., Peng, H., Mu, D., Zhao, H., & Hu, J. (2018). Simultaneous determination of (*N*-ethyl perfluorooctanesulfonamido ethanol)-based phosphate diester and trimester and their biotransformation to perfluorooctanesulfonate in freshwater sediments. *Environmental Pollution*, *234*, 821–829.

 DOI: 10.1002/ieam.4414